Journal of Testing and Evaluation, Vol. 41, No. 2, 2013
Available online at www.astm.org
doi:10.1520/JTE20120100

Ariel E. Matusevich,[1] *Julio C. Massa,*[2] *and Reinaldo A. Mancini*[3]

Computation and Uncertainty Evaluation of Offset Yield Strength

REFERENCE: Matusevich, Ariel E., Massa, Julio C., and Mancini, Reinaldo A., "Computation and Uncertainty Evaluation of Offset Yield Strength," *Journal of Testing and Evaluation*, Vol. 41, No. 2, 2013, pp. 1–14, doi:10.1520/JTE20120100. ISSN 0090-3973.

ABSTRACT: This paper presents computer procedures for the calculation of offset yield strength (S_y) and for the evaluation of the uncertainty in its computation. Offset yield strength is obtained from the plot of stress-strain data recorded in a tension test, as the stress that corresponds to the intersection between the stress-strain curve and a line parallel to its proportional region (offset by a prescribed strain). In the proposed method, the problem is reduced to finding the point of intersection between two straight lines, one that fits the curve in the neighborhood of the intersection and the offset line. For the fitting of each line, we propose the use of a weighted total least-squares algorithm that takes into account uncertainties in both ordinates and abscissas. The evaluation of the uncertainty associated with S_y, in accordance with the *Guide to the Expression of Uncertainty in Measurement*, considers the correlation between the parameters involved in its calculation. The implementation of these procedures motivated the development of dedicated software for the computation of tensile parameters from tension-test raw data and for the estimation of their associated uncertainties. To validate the program, developed in MATLAB as a standalone application, we used a set of ASCII data curves that have agreed values for the tensile parameters and which are publicly available at the web site of the National Physical Laboratory of the United Kingdom. Using these curves we demonstrate the validity of the proposed method for the computation of S_y; to validate the uncertainty-evaluation procedure, we use the law of propagation of probability distributions through Monte Carlo simulation. The computational tool, whose capabilities are presented in this work, is currently being used at the Laboratory of Mechanical Testing of the National Institute of Industrial Technology (INTI), in Córdoba, Argentina.

KEYWORDS: yield strength, proof stress, uncertainty, software, tension test

Introduction

Offset yield strength (S_y), known as proof stress in European countries, is a measure of yielding widely used for design and specification purposes. This parameter is obtained from the plot of stress-strain data recorded in a tension test, as the stress that corresponds to the intersection between the stress-strain curve and a straight line parallel to another that fits the initial linear portion of the curve; the horizontal distance between both lines, referred to as offset, is prescribed as a percentage of the extensometer gauge length (typically 0.1 % or 0.2 % for metals) [1]. A computer method for the calculation of S_y involves the linear regression of the proportional region of the stress-strain diagram and the fitting of the non-linear zone in the neighborhood of the intersection. Because manufacturers of testing machines usually develop their own software for machine control and processing of test parameters, few algorithms for the computation of S_y are publicly available (see Ref 2, for instance).

Manuscript received April 5, 2012; accepted for publication August 2, 2012; published online January 22, 2013.

[1]Research Engineer, INTI-Córdoba, and Assistant Professor, Departamento de Estructuras, Universidad Nacional de Córdoba, Av. Vélez Sarsfield 1561, Córdoba, X5000JKC, Argentina, e-mail: ariel.matusevich@gmail.com

[2]Professor, Departamento de Estructuras, Universidad Nacional de Córdoba, Av. Vélez Sarsfield 1611, Córdoba, X5016GCA Argentina, e-mail: jmassa@efn.uncor.edu

[3]Head of the Materials Division, INTI-Córdoba, and Assistant Professor, Departamento de Materiales y Tecnología, Universidad Nacional de Córdoba, Av. Vélez Sarsfield 1561, Córdoba, X5000JKC, Argentina, e-mail: rmancini@inti.gob.ar

A result for S_y should be accompanied by a parameter that quantifies the accuracy in its determination. This parameter, which represents the uncertainty associated with the measurement, allows realistic comparison of results from different laboratories, within a laboratory, or with reference values given in specifications or standards. In addition, to comply with the requirements of the International Standard ISO/IEC 17025 [3], accredited laboratories shall estimate the uncertainty of measurement using accepted methods of analysis [3]. The need for an internationally accepted procedure for expressing measurement uncertainty led to the publication of the *Guide to the Expression of Uncertainty in Measurement* [4], hereinafter referred to as the GUM. The GUM proposes a standard procedure, known as the GUM uncertainty framework, mainly devoted to linear (or linearized) measurement models. This framework can be applied to a wide range of problems, but has limitations. Supplement 1 to the GUM gives an alternative procedure based on a Monte Carlo method, that can be applied in cases where the GUM uncertainty framework is not applicable or its validity is not clear [5]. We briefly introduce both alternatives in this work.

To our knowledge, there are only two published approaches on the evaluation of the uncertainty associated with S_y: (i) a simplified methodology for evaluating uncertainties of measurements proposed by Loveday [6], which is addressed in an informative annex of the tensile standard EN-10002-1 [7], and (ii) a method published in the *Manual of Codes of Practice for the Determination of Uncertainties in Mechanical Tests on Metallic Materials*, developed within the European Project UNCERT [8]. Both methods are based on the GUM uncertainty framework.

The simplified methodology for evaluating uncertainties of tension-test parameters is based upon an "error budget" concept that uses tolerances specified in testing and calibration standards. In such an approach, uncertainties are calculated as percentages of the parameters they are associated with (2.3 % for the case of S_y) and can be regarded as upper bound estimations [6].

Code of Practice 7 (CoP 7) of the UNCERT Manual [8] deals with the determination of uncertainties in tensile testing. The procedure given in CoP 7 for the evaluation of the uncertainty in the computation of S_y has flaws; the method takes into account the uncertainties in the estimation of the ordinate intercept and the slope of the straight line that fits the elastic part of the stress-strain diagram, but ignores the correlation between both parameters and does not consider the uncertainty associated with the approximation of the non linear part of the curve. If the tension test is carried out using a computer-controlled testing machine, test parameters are automatically processed by dedicated software; because typical testing-machine programs do not return fitting parameters and their standard deviations, which are essential for uncertainty estimation, the application of CoP 7 requires reanalysis of tension-test raw data. For this reason, CoP 7 also gives guidance on how to calculate S_y from tension-test data [8].

In this work, we present computer procedures for the computation of S_y and for the estimation of the uncertainty in its computation. The calculation of S_y is based on searching a portion of the raw-data curve in the neighborhood of its intersection with the offset line, in which a linear fit is valid. Then, we determine S_y as the point of intersection between two straight lines; for the fitting of each line, we propose the use of a weighted total least-squares algorithm that considers uncertainties in both ordinates and abscissas [9]. To evaluate the uncertainty in the determination of S_y, in accordance with the GUM uncertainty framework, we take into account the uncertainties and correlations between the fitting parameters involved in its calculation. We validate the proposed method following the guidelines of GUM S1, using the method of propagation of probability distributions through Monte Carlo simulation [5].

The implementation of the procedures proposed in this article for computation and uncertainty evaluation of S_y motivated the development of a MATLAB standalone application to post process tension-test raw data, to calculate typical tensile parameters and to estimate their uncertainties. To validate the software, we used reference tension-test curves from several materials, obtained through ASCII files that are publicly available at the website of the National Physical Laboratory of the United Kingdom (NPL) [10]. These datasets, developed for tensile-software validation, were originated in the European-Union-funded project TENSTAND (tensile standard) and represent typical tensile characteristics of a variety of industrially important materials [11]. In this work, we present the validation of the procedure for the determination of S_y.

This paper is organized as follows. First, we present the proposed method for the computation of S_y. After giving an introduction to the estimation of uncertainties according to the GUM, we describe the uncertainty-evaluation procedure for S_y. Then, we present the computational tool that implements the proposed methods. Next, we analyze validation exercises and numerical examples. Finally, we present the conclusions of the paper.

Proposed Procedure for the Computation of Offset Yield Strength

Offset yield strength is the quotient between yield force F_y and the original cross-sectional area A_0 of the test specimen

$$S_y = \frac{F_y}{A_0} \tag{1}$$

Yield force is obtained as the point of intersection between the load-extension curve ($F - \delta$) and a line parallel to its proportional region. In this section, we present a procedure for the computation of F_y, schematized in Fig. 1, that can be summarized as follows:

- Determine the upper limit UL and the lower limit LL that define the proportional part of the load-extension curve.
- Compute the parameters of a line I, $F_I = b_1 + m\,\delta$, that best fits load-extension data in the region delimited by UL and LL.
- Calculate the ordinate intercept of an offset line II, $F_{II} = b_2 + m\,\delta$, drawn at a distance from line I whose horizontal projection is βL_e, where β is typically 0.001 or 0.002 and L_e is the initial gauge length of the extensometer used in the tension test.
- Compute the parameters of a third line III, $F_{III} = b_3 + m_3\,\delta$, that fits a small portion of the load-extension curve in the

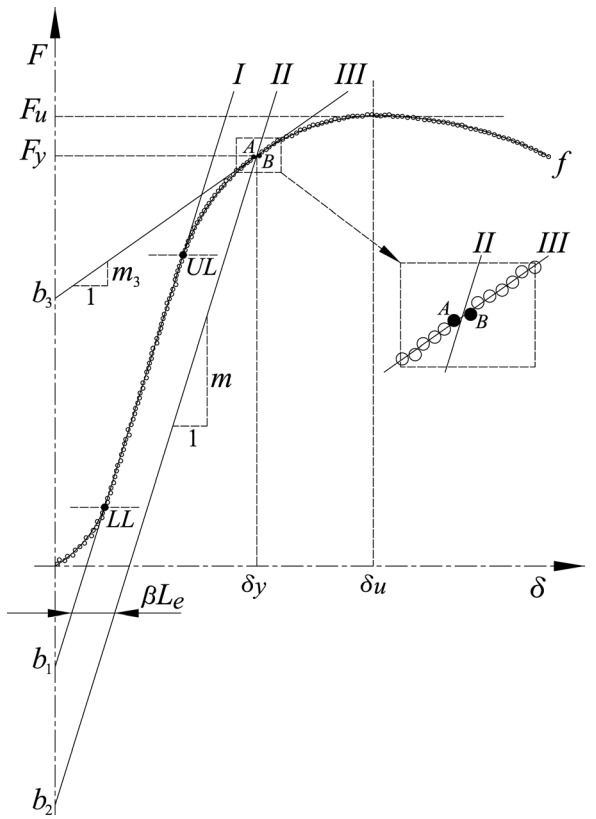

FIG. 1—*Scheme for the computation of F_y.*

neighborhood of its intersection with line *II*, where a linear fit is valid.

- Obtain F_y as the point of intersection between line *II* and line *III*.

In what follows, we detail each of the preceding items.

Upper Limit and Lower Limit of the Proportional Region

The points *UL* and *LL*, shown in Fig. 1, delimit the region of the load-extension curve where data points best seem to follow a straight line. The procedure for the computation of these points, schematized in Fig. 2, is based on a method given in CoP 7 of the UNCERT manual [8]. To reduce the number of calculations in this analysis, we exclude the portion of the F–δ curve beyond the maximum load F_u.

Upper Limit—By removing data pairs in the direction indicated in Fig. 2(*a*), we obtain datasets of decreasing number of experimental points. Using ordinary linear regression, we compute the slopes m of straight lines that fit each set of F–δ data

$$m = \frac{n\sum_{i=1}^{n}\delta_i F_i - \sum_{i=1}^{n}\delta_i \sum_{i=1}^{n}F_i}{n\sum_{i=1}^{n}\delta_i^2 - \left(\sum_{i=1}^{n}\delta_i\right)^2} \tag{2}$$

where n is the number of data pairs. According to CoP 7 [8], we reach the upper limit *UL* when the following ratio results minimum:

$$u_{\text{rel}} = \frac{u(m)}{m} \tag{3}$$

In Eq 3, m is the slope calculated by Eq 2 and $u(m)$ is its standard deviation

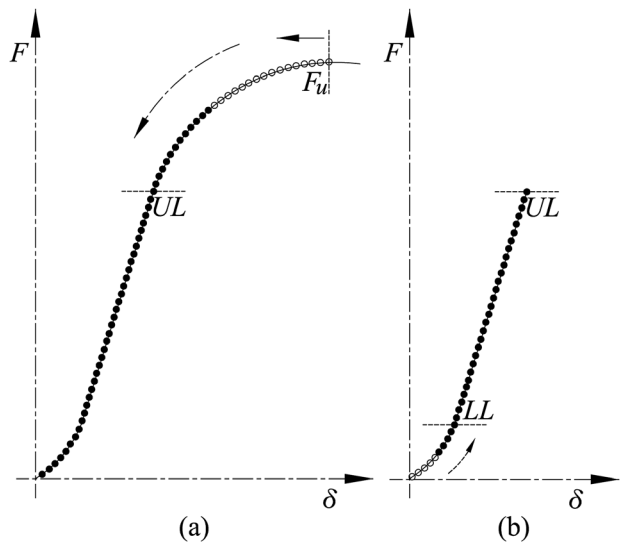

FIG. 2—*Determination of the points that delimit the proportional region.*

$$u(m) = \sqrt{\frac{n\left(\sum_{i=1}^{n}F_i^2 - b\sum_{i=1}^{n}\delta_i F_i\right) - \left(\sum_{i=1}^{n}F_i - b\sum_{i=1}^{n}\delta_i\right)\sum_{i=1}^{n}F_i}{(n-2)\left[n\sum_{i=1}^{n}\delta_i^2 - \left(\sum_{i=1}^{n}\delta_i\right)^2\right]}} \tag{4}$$

where b is the ordinate intercept of the fitted line. In some cases, when anomalies at the start of the tension test occur (these anomalies are typically associated with specimen straightening and initial slackness in the load train), the minimization of Eq 3 leads to the initial segment of the F–δ curve (see Figs. 1 and 2). To avoid this outcome, we propose the minimization of

$$u_{\text{rel}} = \frac{u(m)}{m^2} \tag{5}$$

that discards lines of lower slope.

Lower Limit—Once the upper limit has been determined, we use the same procedure to obtain the lower limit *LL*; in this case, we search for the *LL* in the opposite direction, as indicated in Fig. 2(*b*).

Least-Squares Fitting of the Proportional Region

Force-elongation data within the proportional region is usually fitted by ordinary linear regression. This easy-to-apply technique assumes that abscissas, extension data in our case, are known exactly; because uncertainty associated with extension measurement cannot be considered negligible, this assumption does not hold. On the other hand, the problem of fitting a straight line with errors in both coordinates is not straightforward; it consists in finding the parameters of the line $Y = b + mX$ that minimize the following function [12]:

$$\chi^2 = \sum_{k=1}^{n}\left[\frac{(x_k - X_k)^2}{u_{x,k}^2} + \frac{(y_k - Y_k)^2}{u_{y,k}^2}\right] \tag{6}$$

where (y_k, x_k) denote n given data pairs with estimated standard deviations $(u_{y,k}, u_{x,k})$, whereas (Y_k, X_k) are points of the straight line. In this work, we propose the use of a weighted total least-squares algorithm to solve Eq 6, referred to as WTLS [9], which treats x-and-y data symmetrically. In such a method, the two-dimensional minimization problem is reduced to the one-dimensional search of a minimum, using a different parametrization of the straight line. Krystek and Anton, authors of the WTLS algorithm, have implemented this method as a MATLAB function that can be obtained through the MATLAB Central (File Exchange) [13]. Experimental points (y_k, x_k) and their associated standard deviations $(u_{y,k}, u_{x,k})$ are the input arguments of this function; the program returns the parameters of the fitted line, the minimum value of χ^2 found, and the complete uncertainty matrix, that is, variances and covariance of the fitting parameters. In the WTLS algorithm, the weights associated with data points depend on the standard uncertainties of experimental data; therefore, the effectiveness of the method depends on the correct evaluation of these uncertainties.

TABLE 1—*Uncertainty in force measuring devices (Ref 8).*

Class of Machine	Expanded Uncertainty ($k=2$), U %
0.5	±0.44
1	±0.88
2	±1.75
3	±2.61

Uncertainty in Load-Extension Data—The calibration certificates of the load cell and the extensometer used in the tension test list uncertainties for different ranges of force and extension, respectively. From these certificates we can interpolate the uncertainties ($u_{y,k}$, $u_{x,k}$) that correspond to each data pair (y_k, x_k).

In a simplified approach, we may assume proportional uncertainties for load-and-extension data and use the tolerances of measuring devices specified in standards. Current tensile standards, ASTM E8/E8M-11 [14] and ISO 6892-1 [15], stipulate similar accuracy requirements for the measuring devices involved in the determination of S_y. In this work, we adopt the classifications for testing machines and extensometers given in ISO 7500-1 [16] and ISO 9513 [17], respectively. Tables 1 and 2 list reference tolerances for testing machines and extensometers, extracted from Section 3 of the UNCERT manual [8].

Parameters of the Offset Line

The ordinate intercept of the offset line *II*, drawn at a horizontal distance $\beta\, L_e$ from line *I*, is obtained as follows (see the lower region of Fig. 1):

$$b_2 + m(\beta L_e) = b_1 \rightarrow b_2 = b_1 - m(\beta L_e) \tag{7}$$

Fitting of the F–δ Curve in the Neighborhood of the Intersection

When the fracture point *f* lies below the offset line *II* (see Fig. 1), it is possible to calculate the point of intersection between the offset line and the raw-data curve.

By inspecting experimental points of increasing extension, we search for the first point below the offset line; this point, denoted by $B = (\delta_B, F_B)$, satisfies the following condition:

$$F_B < b_2 + m\,\delta_B \tag{8}$$

The point that immediately precedes point B is designated as $A = (\delta_A, F_A)$; points A and B are shown in the enlarged zone of Fig. 1. We can approximate the nonlinear zone of the raw-data curve by the straight line that passes through points A and B. To improve this rough approximation, we use the WTLS algorithm to obtain the parameters of line *III*, that fits several points on the right of B and on the left of A. To determine the number of data pairs used for fitting line *III*, n_{III}, we use the underlying idea of an algorithm by Goodman et al. [2], that chooses straight line segments by comparing the fits of a straight line and a parabola.

TABLE 2—*Uncertainty in strain measurement using extensometers (Ref 8).*

Class of Extensometer	Expanded Uncertainty ($k=2$), U %
0.2	±0.2
0.5	±0.5
1	±1.0
2	±2.0

Determination of n_{III}—We add n_p points on the right of B and n_p points on the left of A to obtain datasets of increasing number of points

$$n_{III} = 2 + 2n_p \tag{9}$$

Using ordinary least squares, we fit each of the resulting datasets by a straight line and a parabola. To compare both fits, we calculate the mean square error of the linear fit, MSE_l

$$\mathrm{MSE}_l = \frac{1}{n-2}\sum_{i=1}^{n}\left[(b_l + m_l\delta_i) - F_i\right]^2 \tag{10}$$

and the mean square error of the quadratic fit, MSE_q

$$\mathrm{MSE}_q = \frac{1}{n-3}\sum_{i=1}^{n}\left[\left(b_q + m_q\delta_i + c_q\delta_i^2\right) - F_i\right]^2 \tag{11}$$

When the portion of the curve under analysis is close to linear, the gain in accuracy of fit by using a parabola will be small and the quadratic term c_q in the fitted polynomial will be close to zero. Sometimes, a linear fit may be as good or better than a quadratic fit and consequently,

$$\mathrm{MSE}_l \le \mathrm{MSE}_q \quad \rightarrow \quad \frac{\mathrm{MSE}_q}{\mathrm{MSE}_l} \ge 1 \tag{12}$$

which is mathematically possible because the denominator of MSE_l is larger than the denominator of MSE_q. If we denote $R = \mathrm{MSE}_q/\mathrm{MSE}_l$, fitted data can be considered essentially linear whenever $R \ge 1$ [2].

In the proposed method for the determination of n_{III}, we consider $2 \le n_p \le 15$ and pick the value of n_p that gives the longer interval with $R \ge 1$; otherwise, we choose $n_p = 2$ ($n_{III} = 6$).

Point of Intersection

To obtain yield extension δ_y, we set the equation of line *II* equal to the equation of line *III* and solve for δ

$$b_2 + m\delta_y = b_3 + m_3\,\delta_y \rightarrow \delta_y = \frac{b_3 - b_2}{m - m_3} \tag{13}$$

After replacing Eq 7 into Eq 13, we calculate yield force F_y as follows:

$$II(\delta_y) = III(\delta_y) = F_y \rightarrow F_y = \frac{mb_3 - m_3b_1 + \beta\, mm_3L_e}{m - m_3} \tag{14}$$

As Eq 14 indicates, five parameters, b_1, b_3, m, m_3, and L_e are involved in the computation of F_y.

Introduction to Uncertainty Estimation According to the GUM

The standard uncertainty $u(y)$ associated with the measurement result y of a quantity Y is a parameter that characterizes the

dispersion of the values that could reasonably be attributed to Y, expressed as a standard deviation [4].

Uncertainty evaluation involves the use of a model to represent our knowledge about the measurement process. The model relates the quantity subject to measurement, Y, referred to as measurand, and input quantities $X_1, X_2, \ldots, X_N$

$$Y = f_m(X_1, X_2, \ldots, X_N) \tag{15}$$

To express information, usually incomplete, about input contributions, the model formulation involves assignment of probability density functions (PDFs) to input quantities

$$g_{X_1}(\xi_1),\ g_{X_2}(\xi_2), \ldots,\ g_{X_N}(\xi_N) \tag{16}$$

where $\xi_1, \xi_2, \ldots, \xi_N$ represent possible values of $X_1, X_2, \ldots, X_N$, respectively. In the GUM approach, the best estimates x_i of input quantities are the expected values of X_i, where $i = 1, 2, \ldots, N$.

As part of the measurement process, we estimate standard uncertainties $u(x_1), u(x_2), \ldots, u(x_N)$, and covariances $u(x_i, x_j)$, $i \neq j$, associated with input contributions. If uncertainties $u(x_i)$ are estimated by statistical means from a number of repeated observations of X_i, they are designated as Type A according to the GUM; if they are evaluated by any other means (e.g., extracted from a calibration report, or estimated based on past experience) they are classified as Type B.

In general, the aims of a measurement process are: (i) the estimation of the expected value y of Y, (ii) the evaluation of the standard uncertainty $u(y)$ associated with the expected value, and (iii) the determination of the lower limit and the higher limit of an interval (expanded uncertainty) that can be expected to contain a large prescribed portion of the values that can reasonably be attributed to Y. To achieve these goals, the GUM proposes a framework based on the law of propagation of uncertainty, whereas its supplement 1 (GUM S1) uses the method of propagation of probability distributions through Monte Carlo simulation; both approaches are briefly discussed next.

Propagation of Uncertainty

Because the model given by Eq 15 is also valid for estimated quantities, the measurement result y is obtained as

$$y = f_m(x_1, x_2, \ldots, x_N) \tag{17}$$

To evaluate the uncertainty $u(y)$ associated with y, the GUM proposes the use of the law of propagation of uncertainty

$$u(y) = \sqrt{\sum_{i=1}^{N}\left[\frac{\partial f_m}{\partial x_i}u(x_i)\right]^2 + 2\sum_{i=1}^{N-1}\sum_{j=i+1}^{N}\frac{\partial f_m}{\partial x_i}\frac{\partial f_m}{\partial x_j}u(x_i, x_j)} \tag{18}$$

based on a first-order Taylor series expansion of the measurement model, valid when Eq 15 is either linear or can be approximated by a linear function. The partial derivatives in Eq 18 are usually referred to as sensitivity coefficients and are denoted by c_{x_i}, where $i = 1, 2, \ldots, N$.

The computation of expanded uncertainty requires the use of the PDF of the output quantity. Instead of calculating the output PDF explicitly, the GUM uncertainty framework, based on the Central Limit Theorem, assumes that the output PDF is either Gaussian or a t-distribution. The expanded uncertainty U is calculated as

$$U = ku(y) \tag{19}$$

so that the interval $[y - U, y + U]$ has a prescribed coverage probability of the output distribution. The parameter k in Eq 19, known as coverage factor, takes a value of 2 for the case of a normal output distribution and a coverage probability of 95.45 %. The GUM gives a procedure to calculate k, based on the estimation of the (effective) degrees of freedom of input quantities, through the Welch-Satterthwaite equation [4]; however, the procedure has inconsistencies and limitations [18–20].

To illustrate the GUM uncertainty framework we present the diagram of Fig. 3, extracted from the excellent work by Sommer and Siebert on modeling of measurements for uncertainty evaluation [21].

Propagation of Probability Distributions

As Fig. 4 illustrates, the PDFs assigned to input quantities can be propagated through the measurement model to obtain the PDF of the output quantity Y, $g_Y(\eta)$.

Because the propagation of distributions can be carried out analytically only in special cases, it is often implemented using a Monte Carlo method (MCM) [22]. The MCM performs a characterization of the input quantities based on the random sampling of their associated probability density functions; GUM S1 provides specific details of the method and examples of its application [5]. A step-by-step procedure of the method can be summarized as follows [23].

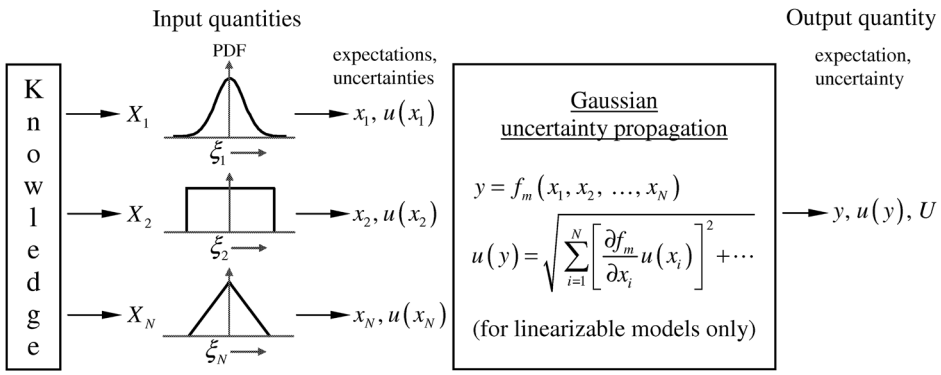

FIG. 3—*Illustration of the GUM uncertainty framework.*

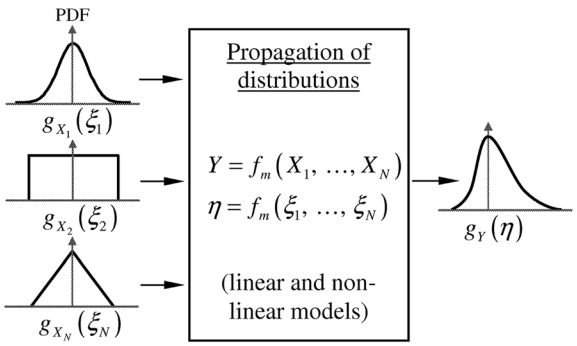

FIG. 4—*Illustration of the propagation of probability distributions.*

- Select the number M of Monte Carlo trials to be made.
- By performing a random sampling of the PDF of each input quantity, obtain a set of M vectors $\{(\xi_1^1, \ldots, \xi_N^1), \ldots, (\xi_1^M, \ldots, \xi_N^M)\}$, where ξ_i^j is the jth random sample of ξ_i.
- Use the model to compute a set $\{\eta^1 = f_m(\xi_1^1, \ldots, \xi_N^1), \ldots, \eta^M = f_m(\xi_1^M, \ldots, \xi_N^M)\}$ of independent random samples of the output PDF, $g_Y(\eta)$.
- Calculate the estimate y and the standard uncertainty $u(y)$ of the output quantity Y as the arithmetic mean and the standard deviation of $\{\eta^1, \ldots, \eta^M\}$, respectively.
- Sort the model values $\{\eta^1, \ldots, \eta^M\}$ in increasing order, $\eta^{(1)} \le \ldots \le \eta^{(M)}$, and use the sorted values to determine the (probabilistically symmetric or shortest) coverage interval $[\eta^{(L)}, \eta^{(H)}]$ at a coverage probability p, where $H - L$ equals the integer part of $pM + \frac{1}{2}$.

Validation of the GUM Uncertainty Framework

Although the GUM uncertainty framework works well in many situations, the applicability of the method depends most notably on

- a valid linear characterization of the model through a first order Taylor approximation,
- the applicability of the Welch-Satterthwaite formula [4] for the estimation of effective degrees of freedom, and
- the assumption that the probability distribution for the output quantity is either Gaussian or a scaled and shifted t-distribution.

Because the method of propagation of distributions through Monte Carlo simulation does not have these limitations, it can be used to validate procedures for uncertainty evaluation that are based on the GUM uncertainty framework. In the validation procedure, we determine whether the interval $[y - U, y + U]$, calculated through the GUM uncertainty framework, agrees with the coverage interval $[\eta^{(L)}, \eta^{(H)}]$ provided by a Monte Carlo method, to a stipulated comparison accuracy ε. When the following conditions are satisfied:

$$d_{\text{low}} = \left|(y - U) - \eta^{(L)}\right| \le \varepsilon \tag{20}$$

$$d_{\text{high}} = \left|(y + U) - \eta^{(H)}\right| \le \varepsilon \tag{21}$$

the comparison is successful and the GUM uncertainty framework has been validated in this instance [5]. The numerical tolerance ε in Eqs 20 and 21 depends on the number n_{dig} of significant digits regarded as meaningful in the numerical value of $u(y)$; usually, $n_{\text{dig}} = 1$ or $n_{\text{dig}} = 2$. To determine ε, we express the value of $u(y)$ in the form $c \times 10^l$, where c is an n_{dig}-digit integer and l is an integer; then, we calculate the comparison accuracy as follows [5]:

$$\varepsilon = \frac{1}{2} 10^l \tag{22}$$

Uncertainty in the Computation of Offset Yield Strength

Using Eqs 1 and 14, we obtain the following mathematical model for the computation of offset yield strength:

$$S_y = \frac{F_y}{A_0}, \quad \text{where} \quad F_y = (mb_3 - m_3 b_1 + \beta\, mm_3 L_e)/(m - m_3) \tag{23}$$

As Eq 23 indicates, the proposed model depends on the parameters of lines *II* and *III*, L_e, and A_0. Measurements of force and extension influence the computation of the parameters of lines *II* and *III*; in fact, the WTLS algorithm requires the estimation of the standard uncertainties associated with ordinates and abscissas, force and extension, respectively.

Other sources that influence force-extension recordings do not appear explicitly in the model equation and are difficult to quantify; they include:

- the alignment of the test specimen, that affects the resulting slope m of the proportional part of the force-extension diagram [24],
- testing-machine characteristics (e.g., stiffness, method and control of operation), and
- speed of testing (within the range allowed in the corresponding tensile standard).

The application of Eq 18 for the evaluation of the standard uncertainty $u(S_y)$ leads to

$$u(S_y) = \sqrt{[c_{F_y} u(F_y)]^2 + [c_{A_0} u(A_0)]^2} \tag{24}$$

because F_y and A_0 are uncorrelated. The sensitivity coefficients in Eq 24 are

$$c_{F_y} = \frac{\partial S_y}{\partial F_y} = \frac{1}{A_0}, \quad c_{A_0} = \frac{\partial S_y}{\partial A_0} = \frac{-F_y}{A_0^2} \tag{25}$$

If additional sources of uncertainty (that do not appear in the model equation) were evaluated, their squared standard uncertainties (variances) could be added inside the square root in Eq 24 [4].

To calculate expanded uncertainty U at a coverage probability of 95.45 %, we assume that the output PDF is Gaussian and use Eq 19 with $k = 2$.

The remainder of this section is devoted to the evaluation of the uncertainties associated with the input quantities indicated in Eq 24.

Uncertainty in the Computation of F_y

To apply the law of propagation of uncertainty for the case of Eq 14, we must consider the mutual correlation between slope and ordinate intercept in line *II* and also in line *III*

$$u(F_y) = \sqrt{\begin{aligned}&[c_{b_1}u(b_1)]^2+[c_m u(m)]^2\\&+[c_{b_3}u(b_3)]^2+[c_{m_3}u(m_3)]^2\\&+[c_{L_e}u(L_e)]^2+2c_{b_1}c_m u(b_1,m)+2c_{b_3}c_{m_3}u(b_3,m_3)\end{aligned}} \tag{26}$$

The sensitivity coefficients in Eq 26 are given by the following expressions:

$$c_{b_1} = \frac{\partial F_y}{\partial b_1} = \frac{-m_3}{m-m_3} \tag{27}$$

$$c_m = \frac{\partial F_y}{\partial m} = \frac{m_3(b_1-b_3-\beta L_e m_3)}{(m-m_3)^2} \tag{28}$$

$$c_{b_3} = \frac{\partial F_y}{\partial b_3} = \frac{m}{m-m_3} \tag{29}$$

$$c_{m_3} = \frac{\partial F_y}{\partial m_3} = \frac{m(b_3-b_1+\beta L_e m)}{(m-m_3)^2} \tag{30}$$

$$c_{L_e} = \frac{\partial F_y}{\partial L_e} = \beta\frac{mm_3}{m-m_3} \tag{31}$$

Uncertainty in the Computation of the Parameters of Lines II and III—The uncertainty matrix associated with the fitting parameters of a straight line $F = b + m\delta$ is

$$\mathbf{\Sigma} = \begin{bmatrix} u^2(m) & u(m,b) \\ u(m,b) & u^2(b) \end{bmatrix} \tag{32}$$

where u^2 denotes variance (square of standard uncertainty) and $u(m, b)$ is the covariance of the fitting parameters m and b. For the case of the WTLS algorithm, the procedure for the evaluation of Eq 32 can be found in Ref 9. The MATLAB function programmed by the authors of the WTLS algorithm, publicly available at the MATLAB Central [13], returns the parameters of the fitted line with their variances and covariance. Our program for the computation of S_y and its uncertainty includes the cited function as a subroutine.

Uncertainty in L_e—To estimate the standard uncertainty in the initial length of the extensometer we consider two contributions: (i) a relative standard uncertainty of ±0.5 % associated with a Class 1 extensometer (see Table 2), and (ii) a relative error of ±1 % attributed to the positioning of the extensometer on the test specimen

$$u(L_e) = \sqrt{(0.005L_e)^2+\left(\frac{0.01L_e}{\sqrt{3}}\right)^2} \tag{33}$$

In Eq 33, we have assumed a rectangular PDF for the distribution of the error associated with the positioning of the extensometer.

Uncertainty in the Calculation of the Initial Cross-Sectional Area A_0

Determination of the initial cross-sectional area requires the measurement of specific dimensions of the test specimen using appropriate instruments. We can identify Type A sources of uncertainty involved in the measurement of the test-specimen dimensions and Type B contributions related to the calibration of measuring instruments. The computation of A_0 and the evaluation of its standard uncertainty involve the following steps.

I. Find the mathematical expression that relates specimen dimensions (input quantities) and A_0 (measurand)

$$A_0 = f_m(X_1, X_2, \ldots, X_N) \tag{34}$$

For the case of a specimen with rectangular cross-sectional area, the required dimensions are the width w and the height h of the specimen reduced section; the relation between the input quantities and the measurand is $A_0 = w \cdot h$.

II. To calculate cross-sectional area, determine the estimates of input quantities x_i as mean values of n measurements

$$x_i = \bar{x}_i = \frac{1}{n}\sum_{k=1}^{n} x_{i_k} \tag{35}$$

with $n \geq 3$.

III. Use the law of propagation of uncertainty given by Eq 18 to compute the combined standard uncertainty associated with the measurement of A_0

$$u(A_0) = \sqrt{[c_{x_1}u(x_1)]^2+\cdots+[c_{x_N}u(x_N)]^2} \tag{36}$$

In Eq 36, we have assumed that input quantities are independent. However, if we use the same instrument to measure two or more dimensions of the test specimen, the resulting estimates are correlated; however, the degree of correlation is usually small and can be safely ignored [25]. To evaluate the standard uncertainties $u(x_i)$ in Eq 36, we use the following procedure:

I. For each input dimension, compute standard deviation

$$s(x_i) = \sqrt{\frac{1}{n-1}\sum_{k=1}^{n}(x_{i_k}-\bar{x}_i)^2} \tag{37}$$

and experimental standard deviation

$$s(\bar{x}_i) = t\frac{s(x_i)}{\sqrt{n}} \tag{38}$$

where t is the student t factor that corresponds to a level of confidence of 68.27 % (one standard deviation).

II. Estimate the standard uncertainty u_{CAL} of the instrument used in the measurement of x_i, from its certificate of calibration.

III. Combine the uncertainties obtained in steps (i) and (ii) to obtain $u(x_i)$.

$$u(x_i) = \sqrt{s^2(\bar{x}_i)+(u_{\mathrm{CAL}})^2} \tag{39}$$

If no information about the measurement process is available, we assume that A_0 has been determined with an accuracy of ±1 % to comply with the requirements of ASTM E8-11 [14] or ISO 6892-1 [15]; considering a level of confidence of 95.45 % ($k = 2$) for this requirement, we obtain

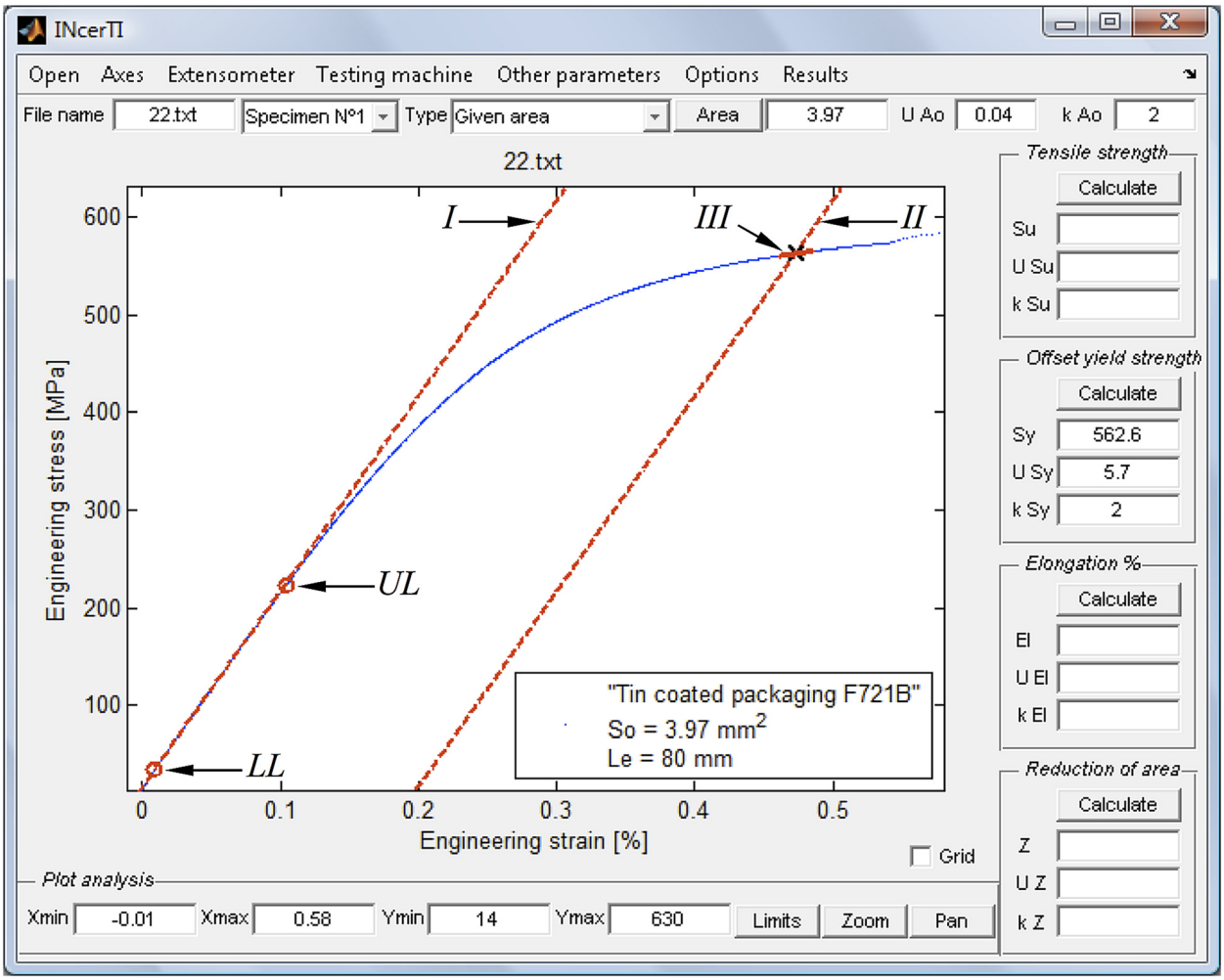

FIG. 5—*Main command window of INcerTI.*

$$u(A_0) = 0.005A_0 \tag{40}$$

Computer Implementation

In this section, we describe the main features of the program INcerTI, developed for the computation of tension-test parameters and for the estimation of their associated uncertainties. The name INcerTI is a play on the Spanish word for uncertainty (incertidumbre) and INTI (Instituto Nacional de Tecnología Industrial) [26], the institution that supported the project. This computational tool was developed in the MATLAB programming language [27] as a standalone application and does not require MATLAB to be installed in the system. INcerTI is run through the graphical user interface shown in Fig. 5.

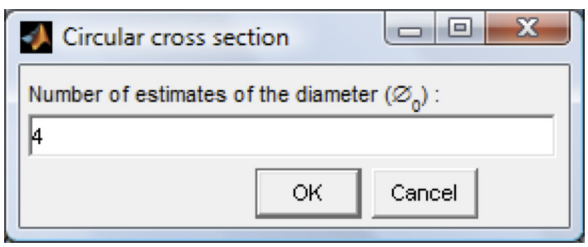

FIG. 6—*Input of the number of diameter estimates.*

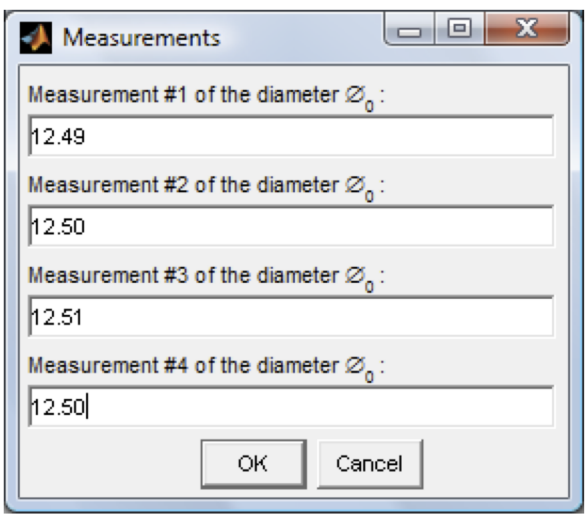

FIG. 7—*Input of diameter estimates.*

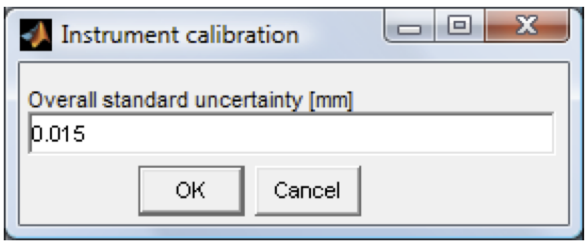

FIG. 8—*Uncertainty of the measuring instrument.*

INcerTI enables the calculation and the uncertainty evaluation of the following tensile parameters: (i) tensile strength, (ii) offset yield strength, (iii) yield points (if they were present), (iv) yield strength for a specified total extension (extension-under-load method), (v) percentage elongation after fracture, (vi) percentage reduction of area (for specimens of circular cross section), and (vii) tensile strain-hardening exponents (n values). In what follows we describe the stages required for the computation of S_y.

Data Input

Computer controlled testing machines typically employ a dedicated software that stores test data and force-extension recordings in text files. To process tensile parameters, INcerTI is capable of reading force-extension recordings from three types of files: (i) ASCII files produced by Series IX software from INSTRON (which controls the testing machine in our laboratory), (ii) standard spreadsheets, and (iii) ASCII validation files, available at the web site of NPL [10]. We use the "Open" menu to locate and load files; the corresponding force-extension diagram is plotted in the command window once the file has been loaded. To examine different regions of the diagram and interpret results, the tools "Zoom," "Pan," and "Limits" are very useful (see the "Plot-analysis" panel at the bottom of the command window in Fig. 5). Using the "Axes" menu, we can change the axes of the diagram between force–extension, force–strain or stress-strain.

Determination of Cross-Sectional Area

To determine the cross-sectional area and its uncertainty, we select the type of specimen using the "Type" pop-up menu (see Fig. 5). Available options include: unmachined test pieces, machined specimens whose cross-sectional area may be circular, annular, or rectangular, and tension specimens taken from large-diameter tubular products. When we click the "Area" button, the program asks for information about the measurement process in an interactive way, then computes cross-sectional area and its uncertainty. Figures 6–8 show the interactive input of data for the case of a test piece of circular cross section whose diameter has been measured four times using a caliper.

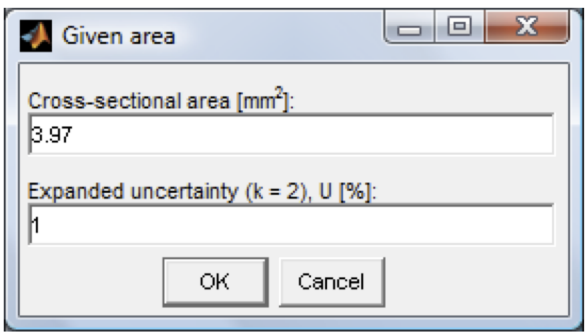

FIG. 9—*Input of a given cross-sectional area.*

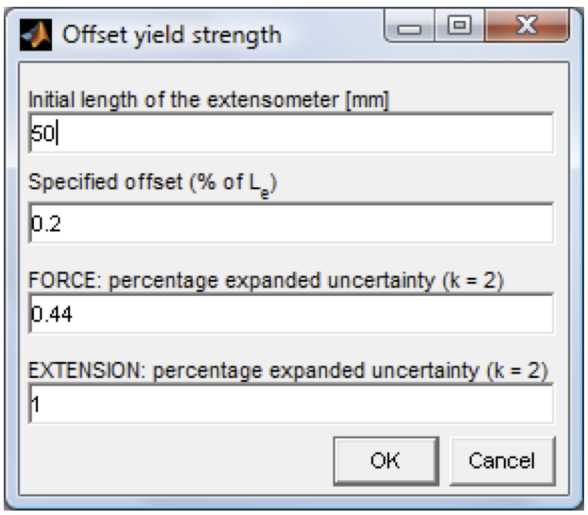

FIG. 10—*Data input for the computation of offset yield strength.*

When cross-sectional area is given with no accompanying information about its estimation, we choose the "Given area" option available in the "Type" pop-up menu; then, after clicking the "Area" button we input cross-sectional area and an estimate of the accuracy in its determination, as Fig. 9 illustrates.

Computation of Offset Yield Strength

The proposed method for the computation of S_y requires the estimation of the standard uncertainties associated with force-extension data; INcerTI provides two methods for the evaluation of these uncertainties, which can be selected through the "Options" menu in the main command window. One method interpolates the uncertainties for each extension-force data pair,

TABLE 3—*Premium quality ASCII datasets.*

TENSTAND Dataset	Material	L_e (mm)	A_0 (mm^2)
1	Nimonic 75, CRM 661	50	78.46
6	Nimonic 75, CRM 661	50	78.54
10	13 % Mn steel	50	77.55
17	316L Stainless steel	50	78.65
22	Tin coated packaging steel	80	3.97
30	Sheet steel—DX56	80	14.17
38	Aluminum sheet—soft AA5182	80	4.62
42	Aluminum sheet—soft AA1050	80	14.48
46	Aluminum sheet—soft AA5182	80	29.59
50	Sheet steel—DX56	50	8.77
57	Synthetic digital curve—zero noise	50	78.54
61	Synthetic digital curve—0.5 % noise	50	78.54
63	Synthetic digital curve—1 % noise	50	78.54

TABLE 4—*Procedure validation for 0.2 % offset yield strength.*

TENSTAND Dataset	S_y – 0.2 % (MPa) Agreed Values	Case (*a*) $S_y \pm U$	Case (*a*) Difference (%)	Case (*b*) $S_y \pm U$	Case (*b*) Difference (%)
1	309.6 – 310.1	309.6 ± 3.2	0	310.0 ± 3.1	0
6	308.0 – 308.6	308.4 ± 3.1	0	308.8 ± 3.1	0.07
10	337.1 – 337.2	337.0 ± 3.6	−0.02	337.3 ± 3.4	0.02
17	261.0 – 261.2	260.1 ± 2.8	−0.36	261.1 ± 2.7	0
22	562.5 – 564.6	562.7 ± 5.8	0	562.6 ± 5.7	0
30	162.7 – 162.9	162.8 ± 1.7	0	162.8 ± 1.6	0
38	396.4 – 397.1	396.5 ± 4.0	0	396.6 ± 4.0	0
42	30.01 – 30.05	30.08 ± 0.32	0.09	30.08 ± 0.31	0.08
46	134.5 – 134.8	134.4 ± 1.4	–0.09	134.4 ± 1.3	−0.06
50	163.9 – 164.0	163.9 ± 1.7	0	163.9 ± 1.6	0
57	434.3	434.1 ± 4.6	−0.04	434.4 ± 4.4	0.02
61	438.1 – 441.6	434.8 ± 4.4	−0.75	435.0 ± 4.4	−0.70
63	446.5 – 448.2	434.7 ± 4.4	−2.65	434.9 ± 4.4	−2.60

by processing text files that contain actual calibration data from the extensometer and from the testing machine. The other method assumes, in a simplified approach, that uncertainties associated with extension and force are proportional to specified uncertainty tolerances of the extensometer and the testing machine, respectively. When we use the latter method, we specify the class of extensometer and the class of testing machine using the third and fourth menus in the command window (see Fig. 5). The dialog window shown in Fig. 10 appears when we click the "Calculate" button of the offset-yield-strength panel; the percentage uncertainties associated with force and extension correspond to tolerances listed in Tables 1 and 2 for the classes of instruments we have selected, though we can type different values.

Figure 5 illustrates a typical output calculation for offset yield strength. INcerTI shows the resulting values for S_y and its expanded uncertainty in designated boxes in the main screen; in addition, the program draws a graph that includes the following features: (i) the original F–δ diagram, (ii) the line that fits the proportional region of the diagram (line *I*), (iii) two circles that highlight the points *UL* and *LL* that delimit the proportional region, (iv) the offset line (line *II*), the line that approximates the non-proportional region (line *III*), and (v) a cross that indicates the point of intersection between *II* and *III*.

Analysis of Case Studies

To study the validity of the procedure for the computation of S_y, we use a set of ASCII datasets with agreed values for the tensile parameters, developed as part of the TENSTAND project [11]. The set of files covers a range of industrially important materials that include: structural steels, stainless steels, aluminum alloys, tin coated packaging steels, BCR Nimonic 75 tensile reference material (CRM 661), and synthetic datafiles with different levels of noise in force data (0 %, 0.5 %, and 1 %).

TABLE 5—*Procedure validation for 0.1 % offset yield strength.*

TENSTAND Dataset	S_y – 0.2 % (MPa) Agreed Values	Case (*a*) $S_y \pm U$	Case (*a*) Difference (%)	Case (*b*) $S_y \pm U$	Case (*b*) Difference (%)
1	303.4 – 304.5	303.3 ± 3.3	−0.04	304.2 ± 3.1	0
6	300.5 – 301.8	301.3 ± 3.3	0	302.2 ± 3.1	0.14
10	334.5 – 334.9	334.0 ± 3.5	−0.14	335.0 ± 3.4	0.02
17	244.7 – 245.2	243.0 ± 2.7	−0.70	245.0 ± 2.5	0
22	525.6 – 530.6	525.5 ± 6.0	−0.03	525.3 ± 5.6	−0.05
30	157.2 – 157.6	157.5 ± 1.6	0	157.5 ± 1.6	0
38	385.2 – 386.8	385.7 ± 4.0	0	385.7 ± 3.9	0
42	26.48 – 26.55	26.56 ± 0.3	0.06	26.56 ± 0.28	0.05
46	133.4 – 133.9	133.7 ± 1.4	0	134.0 ± 1.3	0.07
50	158.6 –158.7	158.8 ± 1.6	0.05	158.8 ± 1.6	0.06
57	432.4	432.3 ± 4.6	−0.03	432.5 ± 4.4	0.03
61	431.8 – 434.1	432.0 ± 4.4	0	432.2 ± 4.3	0
63	429.6 – 432.7	432.7 ± 4.4	0	432.7 ± 4.3	0

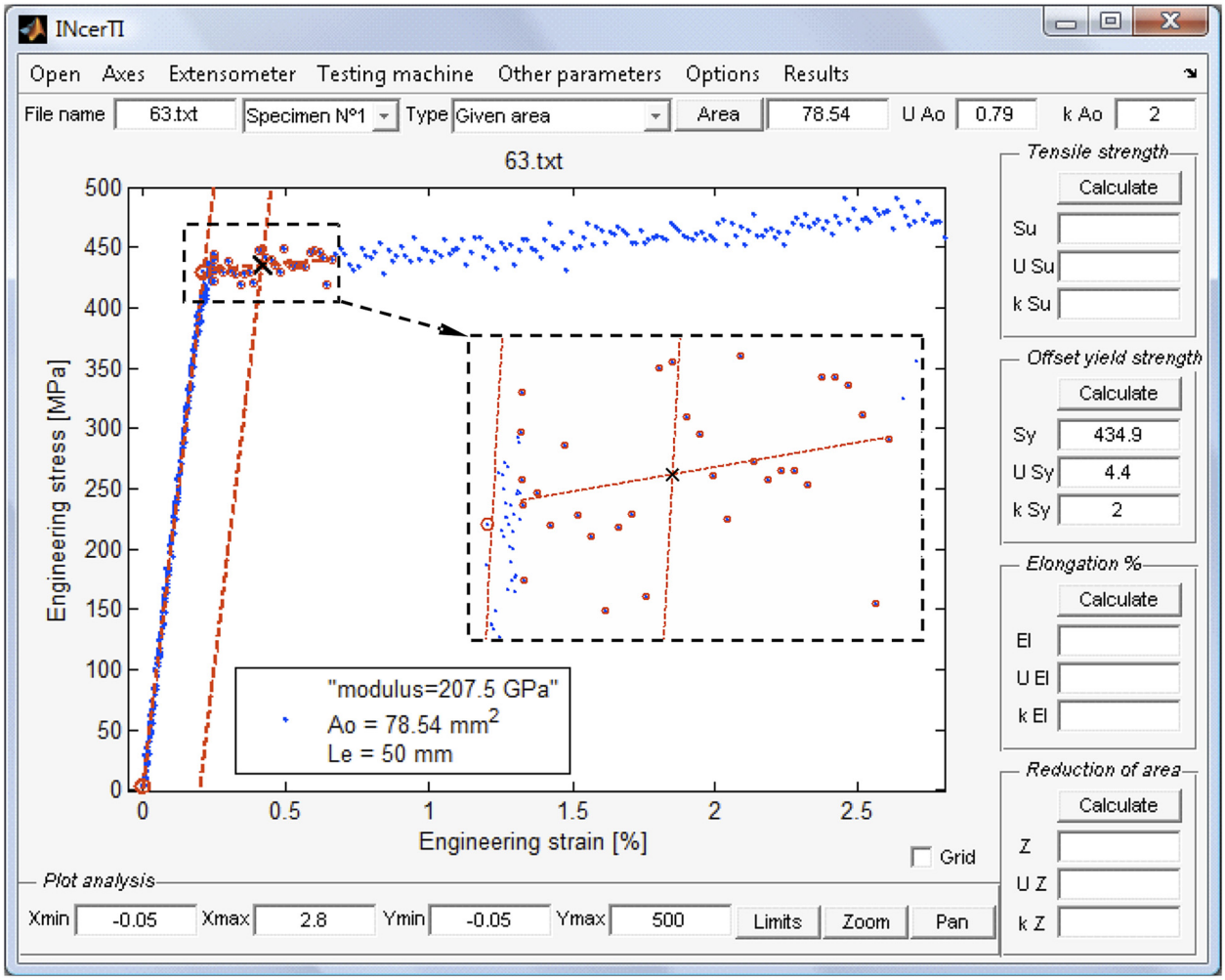

FIG. 11—*Analysis of dataset 63, synthetic file with 1 % noise.*

Table 3 lists details of the thirteen datasets used in the present validation analysis. TENSTAND WP2 Report [11] provides a range of agreed values for S_y (for typical offsets, 0.1 % and 0.2 %) for all the datasets, with the exception of the synthetic file with 0 % noise (dataset 57), where an absolute value could be determined. Results for S_y that lie within the interval or coincide with its boundaries are considered true values.

The methods proposed in this article for the computation of S_y and for the evaluation of its uncertainty require the estimation of the standard uncertainties associated with force-and-elongation

TABLE 6—*Comparison between the GUM uncertainty framework and a Monte Carlo method.*

TENSTAND Dataset	$S_y - 0.2$ % (MPa)	$U(S_y)$ (MPa)	$[S_y - U, S_y + U]$ (MPa)	S_y (MCM) (MPa)	$[\eta^{(L)}, \eta^{(H)}]$ (MPa)	d_{low}	d_{high}
1	309.552	3.151	[306.401, 312.703]	309.560	[306.412, 312.717]	0.01	0.01
6	308.386	3.145	[305.241, 311.531]	308.393	[305.252, 311.543]	0.01	0.01
10	337.039	3.587	[333.452, 340.625]	337.049	[333.460, 340.644]	0.01	0.02
17	260.057	2.840	[257.217, 262.897]	260.059	[257.196, 262.912]	0.02	0.01
22	562.667	5.752	[556.916, 568.419]	562.681	[556.917, 568.441]	0.00	0.02
30	162.813	1.653	[161.160, 164.466]	162.817	[161.163, 164.470]	0.00	0.00
38	396.546	4.030	[392.516, 400.576]	396.558	[392.525, 400.602]	0.01	0.03
42	30.0764	0.317	[29.7594, 30.3934]	30.0771	[29.7599, 30.3942]	0.001	0.001
46	134.385	1.367	[133.019, 135.752]	134.388	[133.024, 135.758]	0.01	0.01
50	163.891	1.664	[162.227, 165.554]	163.894	[162.235, 165.563]	0.01	0.01
57	434.137	4.633	[429.504, 438.770]	434.143	[429.531, 438.804]	0.03	0.03
61	434.806	4.402	[430.404, 439.209]	434.818	[430.408, 439.217]	0.00	0.01
63	434.681	4.401	[430.280, 439.082]	434.690	[430.294, 439.099]	0.01	0.02

TABLE 7—*Fractional uncertainty contributions, file 22, $u(A_0) = 0.005A_0$.*

Offset (% L_e)	S_y (MPa)	U (%)	Percentage Contributions to $u(S_y)$			
			r_{A_0}	r_{L_e}	r_I	r_{III}
0.01	353.4	1.43	48.99	4.46	5.95	40.60
0.02	405.7	1.15	75.08	6.62	3.08	15.22
0.05	477.2	1.08	85.30	5.26	0.57	8.87
0.10	525.3	1.06	89.38	2.93	0.10	7.59
0.20	562.6	1.01	97.80	1.35	0.01	0.83

TABLE 8—*Fractional uncertainty contributions, file 22, $u(A_0) = 0.0025A_0$.*

Offset (% L_e)	S_y (MPa)	U (%)	Percentage Contributions to $u(S_y)$			
			r_{A_0}	r_{L_e}	r_I	r_{III}
0.01	353.4	1.14	19.36	7.05	9.41	64.18
0.02	405.7	0.76	42.96	15.16	7.04	34.84
0.05	477.2	0.65	59.19	14.61	1.59	24.61
0.10	525.3	0.61	67.78	8.89	0.30	23.03
0.20	562.6	0.52	91.76	5.08	0.05	3.11

recordings and information about the measurement of the specimen cross-sectional area. Because TENSTAND documentation does not provide this information, to carry out analyses we make the following considerations based on the fact that the tension tests that produced the datasets were carried out according to EN 10002-1 [7]:

- We evaluate the standard uncertainty associated with the determination of cross-sectional area using Eq 40, which assumes the minimum accuracy required by EN 10002-1 and a normal probability distribution.
- To estimate the standard uncertainties associated with load-and-elongation data we use the tolerances of measuring devices listed in Tables 1 and 2. From all the possible combinations of measuring instruments that comply with EN 10002-1, we analyze two cases, designated as (*a*) and (*b*). In combination (*a*), both the extensometer and testing machine are Class 1 (minimum requirement), whereas in combination (*b*) the extensometer is Class 1 and the testing machine is Class 0.5.

Tables 4 and 5 list results and agreed values for S_y when offsets are 0.2 % and 0.1 %, respectively. In these tables, relative differences between computed results and reference values have been calculated with respect to the nearest limit of the reference interval. All results are accompanied by their expanded uncertainties, for a level of confidence of 95.45 % ($k = 2$).

Computation of 0.2 % Offset Yield Strength

If we exclude from Table 4 the results that correspond to the synthetic files with noise (files 61 and 63), we observe that for combination (*a*) of measuring devices, six values lie within the agreed intervals whereas a maximum difference of 0.36 % is displayed in the case of file 17; for combination (*b*), six results agree with reference values (including file 17) whereas differences in the remaining cases are less than 0.07 %.

Although results for synthetic files 61 and 63 differ significantly from agreed values (almost 3 % for file 63), calculations are very close to the reference value with 0 % noise (file 57); however, the agreed ranges for these curves do not contain the exact result (0 % noise). In Fig. 11, we examine the region of the intersection between the offset line and raw data curve for the case of file 63; data pairs used for the fitting of line *III* are highlighted. Because line *II* crosses a cloud of raw-data points, it is not clear which criterion must be adopted for defining the point of intersection. As the program gave accurate values in all the cases that correspond to actual tension-test recordings, we may conclude that results provided by INcerTI for 0.2 % yield strength are reliable.

Computation of 0.1 % Offset Yield Strength

Table 5 demonstrates the validity of the proposed procedure for the computation of 0.1 % yield strength. Calculated values are accurate in all cases, with the exception of dataset 17; this case exhibits a −0.70 % variation for combination (*a*) of measuring instruments, but the result lies in the middle of the agreed interval for combination (*b*). Small differences in the results can be expected because of the lack of information about the testing machine and extensometer used in each case. Note that agreed values for synthetic files with noise (datasets 61 and 63) do contain the exact result with 0 % noise; in contrast with the agreed intervals that correspond to these datasets for 0.2 % yield strength.

Validation of the Uncertainty-Evaluation Procedure

Through Monte Carlo simulation, we examine the validity of the proposed uncertainty-evaluation procedure; we follow the guidelines that are addressed in a previous section of this paper (Introduction to Uncertainty Estimation According to the GUM).

The MCM requires the random sampling of the PDFs associated with input quantities; for the model of Eq 23, the PDFs include normal distributions assigned to A_0 and L_e and bivariate normal distributions associated with the parameters of lines *II* and *III*. The implementation of the MCM is straightforward in the MATLAB environment, using built-in functions available in the Statistics Toolbox [27].

In the present validation exercise, we consider the computation of 0.2 % yield strength and assume that both the extensometer and the testing machine are Class 1 (combination (*a*) of measuring instruments). We computed the shortest coverage intervals at $p = 0.9545$ for the thirteen datasets, using $M = 9 \times 10^6$ trials in each case. Table 6 lists the coverage intervals given by both methods, the GUM uncertainty framework and the MCM; results are displayed with a high number of significant digits for comparison purposes only. To compare the coverage intervals, we consider $n_{\text{dig}} = 2$ to obtain comparison accuracies according to Eq 22; we use $\varepsilon = 0.005$ MPa for the case of file 42, and $\varepsilon = 0.05$ MPa for the remaining datasets. As Table 6 indicates, the comparison between the GUM uncertainty framework and the MCM is successful for the 13 case studies, because the conditions given by Eq 20 and Eq 21 are satisfied by a safe margin. Although the validation exercise does

not guarantee the validity of the proposed uncertainty-evaluation procedure in all possible cases, the method can be expected to work satisfactorily in situations similar to the ones studied here.

Uncertainty Analysis

To study uncertainty variability in the calculation of S_y, we consider dataset 22 as a case study. To analyze situations where the offset line intersects the raw-data curve in steeper zones, we examine results for five offsets distances from 0.01 % to 0.2 %. To assess the influence of uncertainty components in the evaluation of overall standard uncertainty $u(S_y)$, we compute the fractional contributions of A_0, L_e, line *I*, and line *III*

$$r_{A_0} = \frac{[c_{A_0} u(A_0)]^2}{u^2(S_y)} \tag{41}$$

$$r_{L_e} = \frac{[c_{L_e} u(L_e)]^2}{u^2(S_y)} \tag{42}$$

$$r_I = \frac{[c_{b_1} u(b_1)]^2 + [c_m u(m)]^2 + 2c_{b_1} c_m u(b_1, m)}{u^2(S_y)} \tag{43}$$

$$r_{III} = \frac{[c_{b_3} u(b_3)]^2 + [c_{m_3} u(m_3)]^2 + 2c_{b_3} c_{m_3} u(b_3, m_3)}{u^2(S_y)} \tag{44}$$

that represent variance contributions to total variance. Using options in the "Results" menu of INcerTI, we can visualize fractional uncertainty contributions in the form of pie charts.

Table 7 lists (for five offset distances), results for S_y, their percentage uncertainties U %, and percentage contributions of all components of the uncertainty budget. All cases were calculated using combination (*b*) of measuring instruments (Class 0.5 testing machine and Class 1 extensometer) and assuming the minimum required accuracy in the determination of cross-section area, according to Eq 40. As expected, higher uncertainties are observed for shorter offsets (U varies from 1.43 % to 1.01 %); the calculation of S_y is more sensitive to variations in the parameters of lines *I* and *III* when the offset line intersects the raw-data curve in steeper regions. As Table 7 indicates, the uncertainty in cross-sectional area dominates the uncertainty components. For typical offsets, 0.1 % and 0.2 %, uncertainty in A_0 represents 89.38 % and 97.80 % of the uncertainty budget, respectively. For this reason, the expanded uncertainties listed in Tables 4 and 5 correspond to percentages of calculated values that are between 1 % and 1.1 %. If we examine the results listed in Table 8, where we have assumed that $u(A_0)$ is one half of the tolerance value, percentage uncertainties for S_y vary from 1.14 % to 0.53 % (from the shortest to the longest offset distance); in addition, the fitting of line *III* is the main uncertainty component for the shortest offset, but uncertainty in cross-sectional area dominates for longer offset distances.

Concluding Remarks

We have presented a method for the computation of offset yield strength that adapts features of two published procedures and incorporates the novel use of a weighted total least-squares algorithm for the required fits of force-extension data. Even though the method requires the input of the uncertainties associated with force and extension recordings, we have obtained reliable results for TENSTAND validation files, assuming tolerance values for these uncertainties.

The use of the WTLS algorithm, which takes into account uncertainties in both force and extension, enables a thorough estimation of the uncertainty associated with the calculation of offset yield strength. The proposed uncertainty-estimation procedure, developed according to the GUM uncertainty framework, is expected to give comparable results to those given by a Monte Carlo method. We emphasize that the proposed procedure evaluates the uncertainty associated with the calculation process that leads to the value of S_y, for a given force-extension curve. Although several sources that affect tension-test recordings, and consequently the computed value of S_y, are very difficult to quantify, tensile standards continuously improve test methods to minimize the influence of these sources.

We have shown some capabilities of INcerTI, a dedicated program for post-processing tension-test raw data that integrates, in a novel approach, calculation and uncertainty evaluation of tensile parameters.

Acknowledgments

The authors thank Professors Laura Felicia Matusevich and Michael Anshelevich of Texas A&M University for their help in improving this article. The authors also thank the technicians of the Laboratory of Mechanical Testing of INTI–Córdoba, Julio Costa and Julio Helale, who use the program INcerTI daily, and whose comments have helped us improve this computational tool significantly.

References

[1] Dieter, G., *Mechanical Metallurgy*, McGraw-Hill, New York, 1986, pp. 275–324.

[2] Goodman, M., Jorgensen, J., and Wonsiewicz, B., "Computer-Aided Interpretation of Stress-Strain Curves," *J. Test. Eval.*, Vol. 2, 1974, pp. 361–369.

[3] ISO/IEC 17025, 2005, "General Requirements for the Competence of Testing and Calibration Laboratories," International Organization for Standardization, Geneva, Switzerland.

[4] JCGM 100, 2008, "Evaluation of Measurement Data—Guide to the Expression of Uncertainty in Measurement (GUM 1995 with minor corrections)," http://www.bipm.org/utils/common/documents/jcgm/JCGM_100_2008_E.pdf (Last accessed 28 June 2012).

[5] JCGM 101, 2008, "Evaluation of Measurement Data—Supplement 1 to the 'Guide to the Expression of Uncertainty in Measurement'—Propagation of Distributions Using a Monte Carlo Method," http://www.bipm.org/utils/common/documents/jcgm/JCGM_101_2008_E.pdf (Last accessed 28 June 2012).

[6] Loveday, M. S., "Room Temperature Tensile Testing: A Method for Estimating Uncertainties of Measurement," http://publications.npl.co.uk/npl_web/pdf/cmmt_mn48.pdf (Last accessed 28 June 2012).

[7] EN 10002-1, 2001, "Metallic Materials. Tensile Testing. Part 1: Method of Test at Room Temperature," European Committee for Standardization, Brussels, Belgium.

[8] Kandil, F. A., Gabauer, W., Legendre, L., Brigodiot, G., Tronel, F., Pezzuto, G. F., Plaza, L. M., Foster, D. J., Georgsson, P., Lont, M. A., and Oettel R., 2000, "The UNCERT Manual of Codes of Practice for the Determination of Uncertainties in Mechanical Tests on Metallic Materials," Issue 1, National Physical Laboratory, UK, http://www.npl.co.uk/science-technology/engineered-materials/research/mechanical/uncertainties-in-mechanical-testing-(uncert) (Last accessed 28 June 2012).

[9] Krystek, M. and Anton, M., "A Weighted Total Least-Squares Algorithm for Fitting a Straight Line," *Meas. Sci. Technol.*, Vol. 18, 2007, pp. 3438–3442.

[10] Tensile Testing—Standards and TENSTAND, http://www.npl.co.uk/science-technology/engineered-materials/research/mechanical/tensile-testing-standards-and-tenstand (Last accessed 28 June 2012).

[11] Lord, J., Loveday, M., Rides, M., and McEntaggart, I., 2005, "TENSTAND WP2 Final Report: Digital Tensile Software Evaluation: Computer-Controlled Tensile Testing Machines Validation of European Standard EN 10000-1," National Physical Laboratory, Teddington, http://resource.npl.co.uk/docs/science_technology/materials/measurement_techniques/tenstand/sw_validation_eval.pdf (Last accessed 28 June 2012).

[12] Deming, W. E., *Data Reduction and Error Analysis for the Physical Sciences*, Wiley, New York, 1943.

[13] "Weighted Total Least Squares Straight Line," http://www.mathworks.com/matlabcentral/fileexchange/17466 (Last accessed 28 June 2012).

[14] ASTM E8/E8M-11, 2011, "Standard Test Methods for Tension Testing of Metallic Materials," *Annual Book of ASTM Standards*, Vol. 03.01, ASTM International, West Conshohocken, PA.

[15] ISO 6892-1, 2009, "Metallic Materials—Tensile Testing. Part I: Method of Test at Room Temperature," International Organization for Standardization, Geneva, Switzerland.

[16] ISO 7500-1, 2004, "Metallic Materials—Verification of Static Uniaxial Testing Machines. Part 1: Tension/Compression Testing Machines—Verification and Calibration of the Force-Measuring System," International Organization for Standardization, Geneva, Switzerland.

[17] ISO 9513, 1999, "Metallic Materials—Calibration of Extensometers Used in Uniaxial Testing," International Organization for Standardization, Geneva, Switzerland.

[18] Lepek, A., "A Computer Program for a General Case Evaluation of the Expanded Uncertainty," *Accred. Qual. Assur.*, Vol. 8, 2003, pp. 296–299.

[19] Willink, R., "A Generalization of the Welch-Satterthwaite Formula for Use with Correlated Uncertainty Components," *Metrologia*, Vol. 44, 2007, pp. 340–349.

[20] Willink, R., "An Inconsistency in Uncertainty Analysis Relating to Effective Degrees of Freedom," *Metrologia*, Vol. 45, 2008, pp. 63–67.

[21] Sommer, K. D. and Siebert, B. R. L., "Systematic Approach to the Modelling of Measurements for Uncertainty Evaluation," *Metrologia*, Vol. 43, 2006, pp. S200–S210.

[22] Cox, M. G. and Harris, P. M., "Software Support for Metrology, Best Practice Guide No. 6—Uncertainty Evaluation," *NPL Report DEM-ES-011*, http://publications.npl.co.uk/npl_web/pdf/dem_es11.pdf (Last accessed 28 June 2012).

[23] Wübbeler, G., Krystek, M., and Elster, C., "Evaluation of Measurement Uncertainty and Its Numerical Calculation by a Monte Carlo Method," *Meas. Sci. Technol.*, Vol. 19, 2008, pp. 1–4.

[24] Lord, J. D. and Morrel, R. M., "Elastic Modulus Measurement—Obtaining Reliable Data from the Tensile Test," *Metrologia*, Vol. 47, 2010, pp. S41–S49.

[25] Adams, J., 2002, "G104-A2LA Guide for Estimation of Measurement Uncertainty in Testing," http://www.a2la.org/guidance/est_mu_testing.pdf (Last accessed 28 June 2012).

[26] Instituto Nacional de Tecnología Industrial (INTI), http://www.inti.gob.ar (Last accessed 28 June 2012).

[27] *MathWorks—MATLAB and Simulink for Technical Computing*. http://www.mathworks.com (Last accessed 28 June 2012).

INTERNATIONAL
Standards Worldwide

Address 100 Barr Harbor Drive
PO Box C700
W. Conshohocken, PA
19428-2959 | USA

Phone 610.832.9500
Fax 610.832.9555
e-mail service@astm.org
Web www.astm.org

ERRATUM

JTE20120100, **Computation and Uncertainty Evaluation of Offset Yield Strength**, Ariel E. Matusevich, Julio C. Massa, and Reinaldo A. Mancini, published online in the Journal of Testing and Evaluation (JTE), Volume 41, No. 2, March, 2013.

Page 9, TABLE 3, Row 7, Column 2, *Aluminum sheet—soft AA5182 – should read: Aluminum sheet—hard AA5182.*

Page 10, TABLE 5 heading of Column 2, S_y *– 0.2 % (MPa) Agreed Values* – should read: S_y *– 0.1 % (MPa) Agreed Values.*

Page 11, line 3, *range of agreed values for* S_y – should read: *intervals of agreed values for* S_y.

Page 12, sixth line from bottom, *agreed ranges* – should read: *agreed intervals.*

Page 13, *Acknowledgments*, lines 1 and 3 of the paragraph, *The authors* – should read: *We*.